Engineering Transactions, **71**(4): 645–665, 2023, doi: 10.24423/EngTrans.3107.20231128
Institute of Fundamental Technological Research Polish Academy of Sciences (IPPT PAN)
Université de Lorraine • Poznan University of Technology

Research Paper

Three-Point Bending of a Beam with Non-Homogeneous Structure in the Depth Direction

Krzysztof MAGNUCKI[1)], Ewa MAGNUCKA-BLANDZI[2)], Dawid WITKOWSKI[1)*], Leszek WITTENBECK[2)]

[1)] *Łukasiewicz Research Network – Poznan Institute of Technology Rail Vehicles Center*
Poznan, Poland

[2)] *Institute of Mathematics, Poznan University of Technology*
Poznan, Poland

*Corresponding Author e-mail: dawid.witkowski@pit.lukasiewicz.gov.pl

This paper is devoted to the behavior of a non-homogeneous simply supported beam under three-point bending. The individual shear deformation function of a planar cross-section is adopted, and longitudinal displacements, strains, and stresses for two parts of the beam are explained. By applying the principle of stationary potential energy, a system of two differential equations of equilibrium is derived and solved analytically. The positions of the neutral axis, shear coefficients, and deflections are then calculated for three different beam families. Additionally, the bending problem of these beams is studied numerically using the finite element method (FEM). The results of both analytical and numerical calculations are presented in tables and figures. The main contribution of this paper lies in the development of an analytical model incorporating the individual shear deformation function and a numerical FEM model for this beam.

Keywords: non-homogeneous beam; shear deformation theory; three-point bending.

Notations

x, y, z – Cartesian coordinates,
L – length of the beam,
b – width of the beam,
$h = h_p + h_f$ – total depth of the beam,
$h_p = h_1 + h_2$ – thickness of the upper part,
h_1 – distance from the neutral axis to the upper surface of the beam,

h_2 – distance from the neutral axis to the lower part of the beam,
h_f – thickness of the lower part,
$\chi_1 = h_1/h_p$, $\chi_2 = h_2/h_p$, $\chi_f = h_f/h_p$ – dimensionless coefficients,
k_e, k_s – exponents, positive real numbers,
e_0 – dimensionless coefficient,
$u_1(x)$ – displacement of the lower part of the beam,
$\psi(x) = u_1(x)/h_p$ – dimensionless function,
$v(x)$ – deflection of the beam,
$\eta = y/h_p$ – dimensionless coordinate,
$\xi = x/L$ – dimensionless coordinate,
E_1, E_f – Young's modules of the upper surface and the lower part,
ν – Poisson's ratios of the beam,
$e_f = E_f/E_1$ – dimensionless coefficient,
F – force-load of three-point bending of the beam,
$\lambda = L/h_p$ – relative length of the beam,
$\widetilde{v}_{\max}$ – dimensionless maximum deflection,
C_{se} – shear coefficient of the three-point bending,
$\widetilde{\tau}_{\max}$ – dimensionless maximum shear stress.

1. Introduction

The classic sandwich constructions, which were introduced in the mid-twentieth century, are currently being intensively improved and generalized. Manjunatha and Kant [1] introduced a new set of higher-order theories for analyzing composite and sandwich beams using C^0 finite elements. These theories considered the non-linear variation of displacements throughout the beam thickness, eliminating the need for shear correction coefficients. Their developed computer program incorporated the prediction of interlaminar stresses and demonstrated improved approximation capacity compared to elasticity solutions and classical plate theory, particularly for laminated composite beams ranging from thick to thin. Reddy [2] analyzed functionally graded (FG) plates using the third-order shear deformation plate theory, with the assumption that the modulus of elasticity varied according to a power-law distribution. The finite element models with thermomechanical coupling, time dependency, and von Kármán-type geometric non-linearity were considered. Additionally, Reddy [3] presented theories and associated finite element models for laminated composite structures. Zenkour [4] studied the static response of a simply supported FG rectangular plate subjected to a transverse uniform load by employing the generalized shear deformation theory without transversal shear correction factors, assuming of a power-law distribution of material properties for the plate.

Altenbach and Eremeyev [5] pointed to numerous refinements in plate theory throughout the 20th century and presented an extension of Zhilin's di-

rect approach to plates made of FG materials. Shen [6] discussed the non-linear theory of FG materials. Carrera and Brischetto [7] conducted a comprehensive review of plate theories, including classical, higher order, zigzag, layerwise, and mixed theories, with particular emphasis on the kinematics and numerical assessment of simply supported panels with closed form solutions. The analysis focused on the examination of displacements, stresses, and the free vibration response of simply supported orthotropic panels subjected to a transverse distribution of bisinusoidal pressure. Carrera *et al.* [8] addressed classical and modern beam theories and explored a range of beam problems involving different beam sections across civil and aerospace applications, examining both static and dynamic problems. A refined high-order global-local laminated/sandwich beam theory that satisfies all kinematic and stress continuity conditions at the layer interfaces, was developed in Lezgy-Nazargah *et al.* [9]. Weps *et al.* [10] described the relationships between maximum deflection, transverse shear strain of the core layer, and applied force in a three-point-bending test of laminated beam samples. A comparison was made between the experimentally obtained load-deflection curves and theoretical results obtained through a three-dimensional finite element analysis of three-point-bending for laminated beams.

In Zenkour [11], a refined trigonometric higher-order plate theory was derived, which satisfied free surface conditions, taking into account the effects of transverse shear strains as well as the transverse normal strain. This theory involved only four unknown functions. The bending response of FG rectangular plates was presented, and a comparison was made with corresponding results to check the accuracy and efficiency of the theory. Magnucki *et al.* [12] presented an analytical model of the five-layer sandwich beam and analyzed the influence of the binding layer's thickness and mechanical properties on the beam's deflection under bending. The system of partial differential equations of equilibrium was derived, solved analytically, and a formula describing the beam's deflection was obtained. A comparison of results obtained from analytical and numerical (FEM) analyses was conducted.

Chen *et al.* [13] presented an analysis of the elastic buckling and static bending of shear deformable FG porous beams based on the Timoshenko beam theory. Two different distribution patterns were assumed for the grading of elasticity moduli and mass density of porous composites in the thickness direction. The partial differential equation system governing the buckling and bending behavior of porous beams was derived based on Hamilton's principle. Critical buckling loads and transverse bending deflections were obtained using the Ritz method, where the trial functions were in the form of simple algebraic polynomials. A parametric study was carried out to investigate the effects of the porosity coefficient and slenderness ratio on the buckling and bending characteristics of porous beams. In Sayyad and Ghugal [14], a critical review of literature

was presented, focusing on the bending, buckling and free vibration analysis of shear deformable isotropic, laminated composite and sandwich beams based on equivalent single layer theories, layerwise theories, zig-zag theories and exact elasticity solution. The displacement fields for various equivalent single layer and layerwise theories were summarized.

Vo *et al.* [15] presented a flexural analysis of composite and sandwich beams using a quasi-3D theory, where the axial and transverse displacements were assumed to vary cubically and parabolically through the beam's depth. To address it, two-node C^1 beam elements with six degrees of freedom per node were developed. The effects of fiber angle, lay-up, and span-to-height ratio on displacements and stresses were examined. Abrate and Di Sciuva [16] described an equivalent single-layer theory characterized by a single approximation of the displacements through the thickness. Two broad categories were considered, with the first category expressing the displacement field in terms of polynomial functions of transverse variables, while the second category employing non-polynomial functions. The theories within each category were grouped based on the number of unknown variables to be determined. Magnucka-Blandzi *et al.* [17] analyzed the three-point bending of a simply supported three-layer beam with facings of various thicknesses and various material constants. The analytical model of the beam was formulated, considering a nonlinear hypothesis of deformation of the beam's cross-section. The system of equilibrium equations was derived based on the principle of the total potential energy and analytically solved using trigonometric series. The results were compared with FEM solutions obtained from the SolidWorks Simulation system. Magnucki *et al.* [18] carried out research on a beam with unsymmetrically varying mechanical properties in the depth direction, assuming the nonlinear hypothesis of plane cross-section deformation. Based on Hamilton's principle, two differential equations of motion were obtained. The system of equations was analytically solved in order to analyze bending, buckling, and free vibration problems of the beam. Additionally, an FEM model of the beam was developed, and deflections, critical axial forces, and natural frequencies of the beam were calculated. A comparison was made between the results obtained from these two methods.

Magnucki *et al.* [19] presented an analysis of a rectangular plate with symmetrically varying mechanical properties in the thickness direction. The nonlinear hypothesis of deformation of the straight line normal to the plate neutral surface was assumed. Based on Hamilton's principle, three differential equations of motion were obtained. The system of equations was analytically solved. The critical loads and fundamental natural frequencies for exemplary plates were derived. Furthermore, an FEM model of the plate using the ABAQUS system was developed, and analogical calculations for exemplary plates were performed. The calculation results of these two methods were compared.

Sayyad and Ghugal [20] focused on reviewing research conducted on the modeling and analysis of FG sandwich beams using elasticity theory, analytical methods, and numerical methods based on both classical and refined shear deformation theories. Meksi *et al.* [21] introduced a new shear deformation plate theory to illustrate the bending, buckling, and free vibration responses of FG material sandwich plates. The equations of motion were derived from Hamilton's principle, and analytical solutions for simply supported rectangular sandwich plates were obtained using the Navier solution technique. The influence of critical buckling loads, deflections, stresses, natural frequencies, and sandwich plate type on the bending, buckling, and free vibration responses of FG sandwich plates was examined through a detailed numerical study. Magnucki *et al.* [22] conducted an analysis on an unsymmetrical sandwich beam with varying thicknesses and mechanical properties of the beam faces. A mathematical model of the beam was formulated using the classical broken-line hypothesis. Bending, buckling, and free-vibration were thoroughly studied for exemplary beams. The deflection, critical force, and natural frequency values were determined analytically and compared with those obtained from FEM systems, namely SolidWorks and ABAQUS.

Genovese and Elishakoff [23] discussed the formulation of planar static rod theories, including the effects of transverse shear in a large deformations framework. Furthermore, the differences between Haringx's approach to equilibrium and buckling and Engesser's approach were deliberated. In Magnucki *et al.* [24], two-layer beams with various mechanical properties, thicknesses, and widths of the layers were considered. A novel nonlinear hypothesis-theory of the planar cross-section was developed. In addition, through the principle of stationary potential energy, three differential equations of equilibrium were obtained. The system of equations was analytically solved, and calculations for deflections and normal and shear stresses of exemplary beams were performed. The analytical results were compared with numerical solutions obtained using FEM. Magnucki *et al.* [25] presented simply supported beams under three-point bending with their mechanical properties varying symmetrically in the depth direction. A unique shear deformation theory for beams with such features was proposed. Differential equations of equilibrium were obtained based on the principle of stationary total potential energy. The system of equations was analytically solved, and shear coefficients and deflections of exemplary beams were calculated. The solution was compared with other analytical results obtained using a different deformation function. Furthermore, the bending problem of these beams was numerically studied using FEM.

Malikan and Eremeyev [26] investigated a drawback associated with the material composition of thick functionally graded materials (FGM) beams using a novel hyperbolic-polynomial higher-order elasticity beam theory (HPET).

The proposed beam model incorporated a novel shape function for shear stress deformation distribution and considered the stretching effect caused by thickness variations. The Galerkin method was employed to obtain elastic critical buckling values for different edge conditions. Comparative assessments and validations demonstrated the accuracy and compliance of the proposed shape function. The results highlighted the significant impact of the defect on FGM beams with specific boundary conditions. MALIKAN and EREMEYEV [27] focused on the flexomagnetic (FM) behavior of a vibrating squared multi-physic beam in finite dimensions. The effect of shear deformation's rotary inertia (SDRI) on the FM response was studied in detail, considering the novel concept of rotary inertia from shear deformation. The Galerkin weighted residual technique was used for the solution, and it was observed that SDRI directly affects the FM feature of small-scale actuators.

SEDIGHI *et al.* [28] discussed the use of hybrid nanotubes made of carbon and boron-nitride to exploit the exceptional features of both structures. The nonlocal vibrational behavior of these nano-hetero-tubes in a magneto-thermal environment was studied using a nonlinear finite element formulation. The governing equation of motion was derived based on the adoption of the Euler-Bernoulli beam model and Eringen's nonlocal theory of elasticity. MASJEDI and WEAVER [29] analyzed the deflection of variable stiffness (by fiber steering) composite beams subject to non-uniformly distributed loads. A general analytical solution in integral form was derived and closed-form expressions using series expansion approximations were obtained. GARG *et al.* [30] conducted a comprehensive study on the application of different methods and theories available in the literature for analyzing sandwich FGM structures under different loading conditions. The literature survey included sandwich FGM plates, beams, and shells, including the effects of porosity, hygrothermal loadings, and structures resting on elastic foundations. MAGNUCKI *et al.* [31] presented three models of sandwich beams incorporating the "broken line" and two nonlinear individual shear deformation theories.

The subject of this study is an analysis of a non-homogeneous beam of a length L, total depth h and width b (Fig. 1a). The beam is situated in the Cartesian coordinate system xyz. The mechanical properties of the upper part, with a thickness h_p, are variable, while, in the lower part, the thin-walled face with a thickness h_f, these properties are constant. The three-point bending problem of the beam (Fig. 1b) with consideration given to the shear effect is analytically and numerically (FEM) studied.

Both supports at the beam's ends are positioned in the neutral plane – the neutral axis (Fig. 1b). The position of neutral axis is determined from a condition given in expression (2.15).

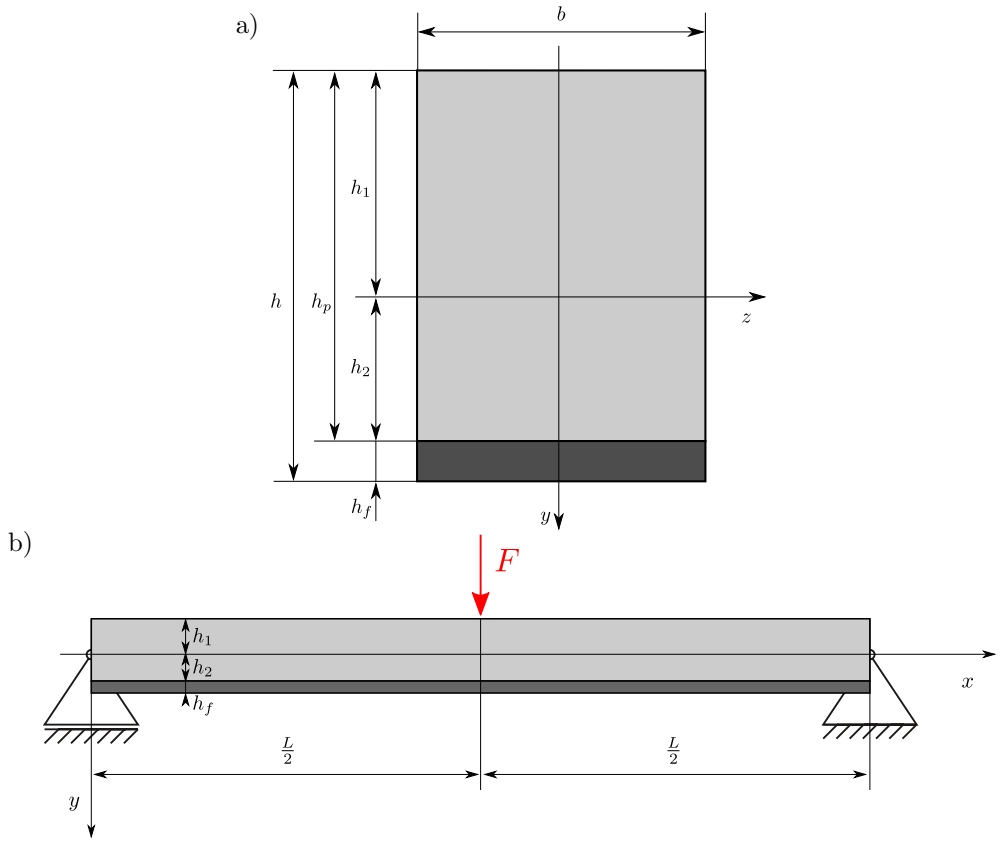

FIG. 1. Schemes of the cross-section and load of the beam: a) the cross-section of the beam, b) load – three-point bending.

2. Analytical model of the beam

The Young's modulus variability in the depth direction of the beam is shown in Fig. 2.

The Young's modulus varies as follows:

- the upper part $(-\chi_1 \leq \eta \leq \chi_2)$

$$E(\eta) = E_1 f_e(\eta), \tag{2.1}$$

where

$$f_e(\eta) = e_0 + (1 - e_0)\left[3(\eta - \chi_2)^4 - 2(\eta - \chi_2)^6\right]^{k_e}, \tag{2.2}$$

and $f_e(\chi_2) = e_0$, $\chi_1 = h_1/h_p$, $\chi_2 = h_2/h_p$ – dimensionless coefficients $(\chi_1 + \chi_2 = 1)$, $\eta = y/h_p$ – dimensionless coordinate, e_0 – dimensionless coefficient, k_e – exponent (positive real number).

- the lower part – the thin-walled face ($\chi_2 \leq \eta \leq \chi_2 + \chi_f$)

$$E(\eta) = E_f = \text{const}, \tag{2.3}$$

where $\chi_f = h_f/h_p$ – dimensionless coefficient – relative thickness of the lower part.

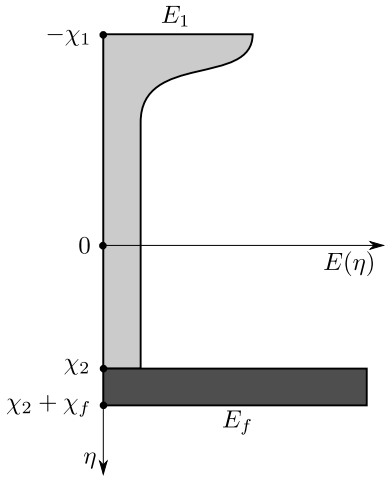

FIG. 2. Scheme of the Young's modulus variability in the depth direction of the beam.

The deformation of the planar cross-section after bending of the beam is shown in Fig. 3.

Taking into account the paper [25], the individual nonlinear dimensionless function of deformation of the planar cross-section of the upper part is assumed in the following form:

$$f_d(\eta) = \frac{1}{C_0} \int \frac{\left[1 - (\eta/\chi_1)^2\right]^{k_s}}{f_e(\eta)} \, \mathrm{d}\eta, \tag{2.4}$$

where $C_0 = \int_{-\chi_1}^{0} \frac{\left[1-(\eta/\chi_1)^2\right]^{k_s}}{f_e(\eta)} \, \mathrm{d}\eta$ – dimensionless coefficient, k_s – exponent (positive real number).

Thus, the derivative of this function is as follows:

$$\frac{\mathrm{d}f_d}{\mathrm{d}\eta} = \frac{1}{C_0} \frac{\left[1 - (\eta/\chi_1)^2\right]^{k_s}}{f_e(\eta)}. \tag{2.5}$$

The function (2.4) and the derivative (2.5) satisfy the conditions: $f_d(-\chi_1) = -1$, $\mathrm{d}f_d/\mathrm{d}\eta|_{-\chi_1} = 0$.

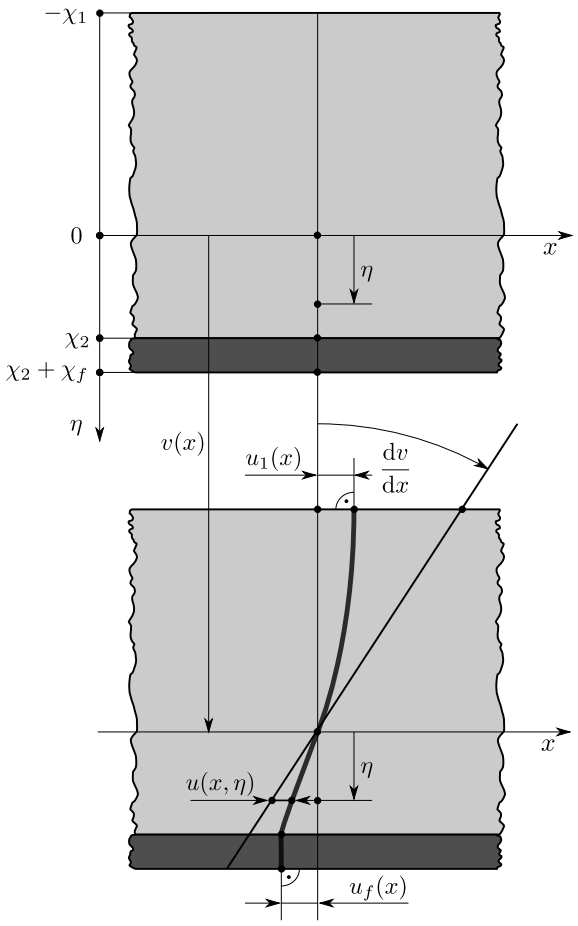

FIG. 3. Scheme of the deformation of the planar cross-section.

The longitudinal displacements are as follows:

- the upper part $(-\chi_1 \leq \eta \leq \chi_2)$

$$u_p(x,\eta) = -h_p\left[\eta\frac{\mathrm{d}v}{\mathrm{d}x} - f_d(\eta)\,\psi(x)\right], \tag{2.6}$$

where $v(x)$ – deflection, $\psi(x) = u_1(x)/h_p$ – dimensionless function.

- the lower part – the thin-walled face $(\chi_2 \leq \eta \leq \chi_2 + \chi_f)$

$$u_f(x,\eta) = -h_p\left[\eta\frac{\mathrm{d}v}{\mathrm{d}x} - C_f\psi(x)\right], \tag{2.7}$$

where $C_f = \dfrac{1}{C_0}\displaystyle\int_0^{\chi_2}\frac{\left[1-(\eta/\chi_1)^2\right]^{k_s}}{f_e(\eta)}\,\mathrm{d}\eta$ – dimensionless coefficient.

Therefore, the strains are:

- the upper part $(-\chi_1 \leq \eta \leq \chi_2)$

$$\begin{aligned} \varepsilon_x^{(p)}(x,\eta) &= \frac{\partial u_p}{\partial x} = -h_p\left[\eta\frac{\mathrm{d}^2 v}{\mathrm{d}x^2} - f_d(\eta)\frac{\mathrm{d}\psi}{\mathrm{d}x}\right], \\ \gamma_{xy}^{(p)}(x,\eta) &= \frac{\mathrm{d}v}{\mathrm{d}x} + \frac{\partial u_p}{h_p \partial \eta} = \frac{\mathrm{d}f_d}{\mathrm{d}\eta}\psi(x), \end{aligned} \tag{2.8}$$

- the lower part – the thin-walled face $(\chi_2 \leq \eta \leq \chi_2 + \chi_f)$

$$\begin{aligned} \varepsilon_x^{(f)}(x,\eta) &= \frac{\partial u_f}{\partial x} = -h_p\left[\eta\frac{\mathrm{d}^2 v}{\mathrm{d}x^2} - C_f\frac{\mathrm{d}\psi}{\mathrm{d}x}\right], \\ \gamma_{xy}^{(f)}(x,\eta) &= \frac{\mathrm{d}v}{\mathrm{d}x} + \frac{\partial u_f}{h_p \partial \eta} = 0. \end{aligned} \tag{2.9}$$

Consequently, the stresses – Hooke's law are:

- the upper part $(-\chi_1 \leq \eta \leq \chi_2)$

$$\begin{aligned} \sigma_x^{(p)}(x,\eta) &= E_1 \varepsilon_x^{(p)}(x,\eta) f_e(\eta), \\ \tau_{xy}^{(p)}(x,\eta) &= \frac{E_1}{2(1+\nu)}\gamma_{xy}^{(p)}(x,\eta) f_e(\eta), \end{aligned} \tag{2.10}$$

  where ν – Poisson ratio is assumed constant for the structures [25].

- the lower part – the thin-walled face $(\chi_2 \leq \eta \leq \chi_2 + \chi_f)$

$$\begin{aligned} \sigma_x^{(f)}(x,\eta) &= E_f \varepsilon_x^{(f)}(x,\eta), \\ \tau_{xy}^{(f)}(x,\eta) &= 0. \end{aligned} \tag{2.11}$$

The bending moment $M_b(x) = \int\limits_A y\sigma_x(x,y)\,\mathrm{d}A$, considering the expressions (2.8), (2.9), (2.10) and (2.11) is as follows:

$$\begin{aligned} M_b(x) = -bh_p^3 \Bigg\{ & E_1 \int\limits_{-\chi_1}^{\chi_2} \left[\eta^2\frac{\mathrm{d}^2 v}{\mathrm{d}x^2} - \eta f_d(\eta)\frac{\mathrm{d}\psi}{\mathrm{d}x}\right] f_e(\eta)\,\mathrm{d}\eta \\ & + E_f \int\limits_{\chi_2}^{\chi_2+\chi_f} \left[\eta^2\frac{\mathrm{d}^2 v}{\mathrm{d}x^2} - C_f\eta\frac{\mathrm{d}\psi}{\mathrm{d}x}\right]\mathrm{d}\eta \Bigg\}. \end{aligned} \tag{2.12}$$

After a simple transformation of this expression, one obtains the equation in the following form:

$$C_{vv}\frac{\mathrm{d}^2 v}{\mathrm{d}x^2} - C_{v\psi}\frac{\mathrm{d}\psi}{\mathrm{d}x} = -\frac{M_b(x)}{E_1 b h_p^3}, \tag{2.13}$$

where

$$C_{vv} = \int_{-\chi_1}^{\chi_2} \eta^2 f_e(\eta)\,\mathrm{d}\eta + \frac{1}{3}e_f\chi_f\left(3\chi_2^2 + 3\chi_2\chi_f + \chi_f^2\right), \quad e_f = E_f/E_1,$$

$$C_{v\psi} = \int_{-\chi_1}^{\chi_2} \eta\, f_e(\eta)\, f_d(\eta)\,\mathrm{d}\eta + \frac{1}{2}C_f\, e_f\, \chi_f\,(2\chi_2 + \chi_f).$$

The axial force $N(x) = \int_A \sigma_x(x,y)\,\mathrm{d}A$, considering the expressions (2.8), (2.9), (2.10) and (2.11) is as follows:

$$N(x) = -bh_p^2\left\{E_1\int_{-\chi_1}^{\chi_2}\left[\eta\frac{\mathrm{d}^2 v}{\mathrm{d}x^2} - f_d(\eta)\frac{\mathrm{d}\psi}{\mathrm{d}x}\right]f_e(\eta)\,\mathrm{d}\eta + E_f\int_{\chi_2}^{\chi_2+\chi_f}\left[\eta\frac{\mathrm{d}^2 v}{\mathrm{d}x^2} - C_f\frac{\mathrm{d}\psi}{\mathrm{d}x}\right]\mathrm{d}\eta\right\}. \tag{2.14}$$

The position of the neutral axis (Fig. 1a) is determined from the condition $N(x) = 0$. Taking into account the paper [24], this condition with simplification relating to the omission of the shear effect is in the following form:

$$E_1\int_{-\chi_1}^{\chi_2}\eta f_e(\eta)\,\mathrm{d}\eta + E_f\int_{\chi_2}^{\chi_2+\chi_f}\eta\,\mathrm{d}\eta = 0. \tag{2.15}$$

Based on this, the value of the dimensionless coefficient χ_2 is calculated.

The elastic strain energy of the beam, considering the expressions (2.8), (2.9), (2.10) and (2.11) is as follows:

$$U_\varepsilon = \frac{1}{2} b \int_0^L \left\{ E_1 h_p^3 \int_{-\chi_1}^{\chi_2} \left[\eta \frac{\mathrm{d}^2 v}{\mathrm{d}x^2} - f_d(\eta) \frac{\mathrm{d}\psi}{\mathrm{d}x} \right]^2 f_e(\eta)\, \mathrm{d}\eta \right. \tag{2.16}$$

$$+ \frac{E_1 h_p}{2(1+\nu)} \frac{\psi^2(x)}{C_0^2} \int_{-\chi_1}^{\chi_2} \frac{\left[1 - (\eta/\chi_1)^2\right]^{2k_s}}{f_e(\eta)} \mathrm{d}\eta$$

$$\left. + E_f h_p^3 \int_{\chi_2}^{\chi_2+\chi_f} \left[\eta \frac{\mathrm{d}^2 v}{\mathrm{d}x^2} - C_f \frac{\mathrm{d}\psi}{\mathrm{d}x} \right]^2 \mathrm{d}\eta \right\} \mathrm{d}x.$$

After a simple transformation, this expression is in the following form:

$$U_\varepsilon = \frac{1}{2} E_1 b h_p^3 \int_0^L \left\{ C_{vv} \left(\frac{\mathrm{d}^2 v}{\mathrm{d}x^2} \right)^2 - 2 C_{v\psi} \frac{\mathrm{d}^2 v}{\mathrm{d}x^2} \frac{\mathrm{d}\psi}{\mathrm{d}x} \right. \tag{2.17}$$

$$\left. + C_{\psi\psi} \left(\frac{\mathrm{d}\psi}{\mathrm{d}x} \right)^2 + \frac{C_\psi}{2(1+\nu)} \frac{\psi^2(x)}{h_p^2} \right\} \mathrm{d}x,$$

where

$$C_{\psi\psi} = \int_{-\chi_1}^{\chi_2} f_e(\eta) f_d^2(\eta)\, \mathrm{d}\eta + C_f^2 e_f \chi_f,$$

$$C_\psi = \frac{1}{C_0^2} \int_{-\chi_1}^{\chi_2} \frac{\left[1 - (\eta/\chi_1)^2\right]^{2k_s}}{f_e(\eta)} \mathrm{d}\eta.$$

Taking into account the paper [25], the work of the load is as follows:

$$W = \int_0^L T(x) \frac{\mathrm{d}v}{\mathrm{d}x}\, \mathrm{d}x, \tag{2.18}$$

where $T(x) = \mathrm{d}M_b/\mathrm{d}x$ – transverse-shear force.

Based on the principle of stationary total potential energy $\delta(U_\varepsilon - W) = 0$, the system of two differential equations of equilibrium for the beam is derived in the following form:

$$E_1 b h_p^3 \left(C_{vv} \frac{\mathrm{d}^4 v}{\mathrm{d}x^4} - C_{v\psi} \frac{\mathrm{d}^3 \psi}{\mathrm{d}x^3} \right) + \frac{\mathrm{d}T}{\mathrm{d}x} = 0, \tag{2.19}$$

$$C_{v\psi} \frac{\mathrm{d}^3 v}{\mathrm{d}x^3} - C_{\psi\psi} \frac{\mathrm{d}^2 \psi}{\mathrm{d}x^2} + \frac{C_\psi}{2(1+\nu)} \frac{\psi(x)}{h_p^2} = 0. \tag{2.20}$$

It is noted that the differential Eqs. (2.13) and (2.19) are equivalent. Thus, Eqs. (2.13) and (2.20) are governing equilibrium equations for the bending beam with a non-homogeneous structure in the depth direction. This system, after transformation, is reduced to one differential equation of second order in the following form:

$$\frac{\mathrm{d}^2\psi}{\mathrm{d}x^2} - \alpha^2 \frac{\psi(x)}{h_p^2} = -\frac{C_{v\psi}}{C_{vv}C_{\psi\psi} - C_{v\psi}^2} \frac{T(x)}{E_1 b h_p^3}, \tag{2.21}$$

where $\alpha = \sqrt{\frac{1}{2(1+\nu)} \frac{C_{vv}C_{\psi}}{C_{vv}C_{\psi\psi} - C_{v\psi}^2}}$ – dimensionless coefficient.

Taking into account the paper [25], this equation in the dimensionless coordinate is as follows:

$$\frac{\mathrm{d}^2\psi}{\mathrm{d}\xi^2} - (\alpha\lambda)^2 \psi(\xi) = -\frac{C_{v\psi}}{C_{vv}C_{\psi\psi} - C_{v\psi}^2} \lambda^2 \frac{T(\xi)}{E_1 b h_p}, \tag{2.22}$$

where $\xi = x/L$ is dimensionless coordinate, and $\lambda = L/h_p$ is relative length of the beam.

3. Analytical study of the three-point bending of the beam

The bending moment and the shear-transverse force of the three-point bending are as follows:

$$M_b(\xi) = \begin{cases} \xi FL/2 & \text{for} \quad 0 \le \xi \le 1/2, \\ (1-\xi) FL/2 & \text{for} \quad 1/2 \le \xi \le 1, \end{cases} \tag{3.1}$$

$$T(\xi) = \begin{cases} F/2 & \text{for} \quad 0 \le \xi < 1/2, \\ 0 & \text{for} \quad \xi = 1/2, \\ -F/2 & \text{for} \quad 1/2 < \xi \le 1. \end{cases} \tag{3.2}$$

The solution to Eq. (2.22), considering the conditions $\mathrm{d}\psi/\mathrm{d}\xi|_0 = 0$, $\mathrm{d}\psi/\mathrm{d}\xi|_1 = 0$, $\psi(1/2) = 0$ and the expression (3.2), is the dimensionless function in the following form:

- for the first interval $(0 \le \xi \le 1/2)$

$$\psi(\xi) = (1+\nu) \left[1 - \frac{\cosh(\alpha\lambda\xi)}{\cosh(\alpha\lambda/2)}\right] \frac{C_{v\psi}}{C_{vv}C_{\psi}} \frac{F}{E_1 b h_p}, \tag{3.3}$$

- for the second interval $(1/2 \le \xi \le 1)$

$$\psi(\xi) = -(1+\nu) \left[1 - \frac{\cosh[\alpha\lambda(1-\xi)]}{\cosh(\alpha\lambda/2)}\right] \frac{C_{v\psi}}{C_{vv}C_{\psi}} \frac{F}{E_1 b h_p}. \tag{3.4}$$

Equation (2.13) after integration, considering the bending moment (3.1) and the dimensionless function (3.3) for the first interval and also the condition $\mathrm{d}\widetilde{v}/\,\mathrm{d}\xi|_{1/2} = 0$, is in the following form:

$$\frac{\mathrm{d}v}{\mathrm{d}\xi} = \left\{(1+\nu)\left[1 - \frac{\cosh(\alpha\lambda\xi)}{\cosh(\alpha\lambda/2)}\right]\frac{C_{v\psi}^2}{C_{vv}C_\psi} + \frac{1}{16}\left(1-4\xi^2\right)\lambda^2\right\}\frac{\lambda}{C_{vv}}\frac{F}{E_1 b}. \tag{3.5}$$

This Eq. (3.5) after integration, considering the condition $\widetilde{v}(0) = 0$, is as follows:

$$v(\xi) = \left\{(1+\nu)\left[\xi - \frac{1}{\alpha\lambda}\frac{\sinh(\alpha\lambda\xi)}{\cosh(\alpha\lambda/2)}\right]\frac{C_{v\psi}^2}{C_{vv}C_\psi} + \frac{1}{16}\left(\xi - \frac{4}{3}\xi^3\right)\lambda^2\right\}\frac{\lambda}{C_{vv}}\frac{F}{E_1 b}. \tag{3.6}$$

Therefore, the maximum deflection of the beam is

$$v_{\max} = v\left(\frac{1}{2}\right) = \widetilde{v}_{\max}\frac{F}{E_1 b}, \tag{3.7}$$

where the dimensionless maximum deflection is

$$\widetilde{v}_{\max} = (1 + C_{se})\frac{\lambda^3}{48 C_{vv}}, \tag{3.8}$$

and the shear coefficient is

$$C_{se} = \max_{k_s}\left\{\frac{24}{\lambda^2}(1+\nu)\left[1 - \frac{2}{\alpha\lambda}\tanh\left(\frac{\alpha\lambda}{2}\right)\right]\frac{C_{v\psi}^2}{C_{vv}C_\psi}\right\}. \tag{3.9}$$

The shear stress (2.10) considering the functions (2.5) and (3.3) is in the following form:

$$\tau_{xy}^{(p)}(\xi,\eta) = \widetilde{\tau}_{xy}^{(p)}(\xi,\eta)\frac{F}{b h_p}. \tag{3.10}$$

where the dimensionless shear stress is defined as:

$$\widetilde{\tau}_{xy}^{(p)}(\xi,\eta) = \frac{1}{2C_0}\left[1 - (\eta/\chi_1)^2\right]^{k_s}\left[1 - \frac{\cosh(\alpha\lambda\xi)}{\cosh(\alpha\lambda/2)}\right]\frac{C_{v\psi}}{C_{vv}C_\psi}. \tag{3.11}$$

Therefore, the maximum of this stress for $\xi = 1/4$ is as follows:

$$\widetilde{\tau}_{\max} = \widetilde{\tau}_{xy}^{(p)}\left(\frac{1}{4}, 0\right) = \frac{1}{2C_0}\left[1 - \frac{\cosh(\alpha\lambda/4)}{\cosh(\alpha\lambda/2)}\right]\frac{C_{v\psi}}{C_{vv}C_\psi}. \tag{3.12}$$

The detailed studies are carried out for a family of three exemplary beams with the following sizes: $b = 20$ mm, $h = 35$ mm, $h_p = 34$ mm, $h_f = 1$ mm, $L = 340, 425, 510$ mm, therefore the dimension length $\lambda = 10.0, 12.5, 15.0$. The variability of the Young's modulus in the depth direction of the three exemplary beams are shown in Fig. 4.

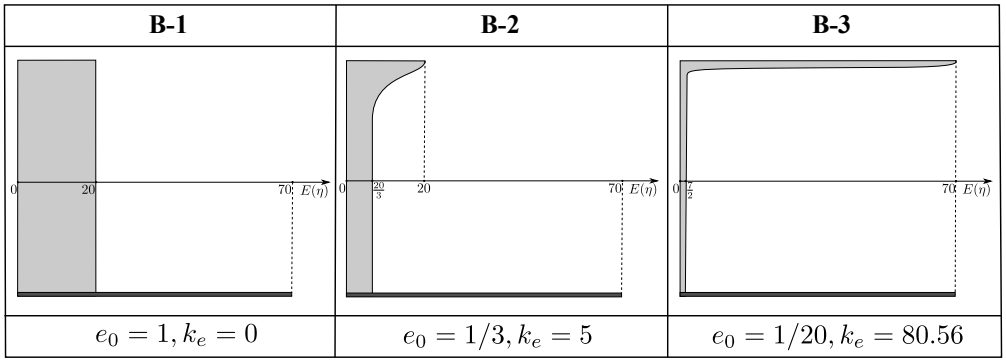

FIG. 4. The graphs of the Young's modulus variability in the depth direction for the exemplary beams.

Examples:

- Beam B-1.

Young's modules of the upper and lower parts are constant: $E_1 = 20$ GPa, $E_f = 70$ GPa, and Poisson ratio is also constant $\nu = 0.3$. Therefore, based on the position of the neutral axis (2.15), the value of the dimensionless coefficient is $\chi_2 = 0.45196$. The results of the calculations are specified in Table 1.

Table 1. The results of the analytical calculations for the exemplary beam B-1.

λ	10.0	12.5	15.0
k_s	0.9276	0.9419	0.9514
C_{se}	0.03742	0.02400	0.01669
$\widetilde{v}_{\max}$	200.00	385.57	661.49
$\widetilde{\tau}_{\max}$	0.6859	0.6877	0.6889

- Beam B-2.

Young's modulus of the upper part of the beam is variable according to the function (2.2) – Fig. 4 ($E_1 = 20$ GPa, $E_f = 70$ GPa , $\nu = 0.3$). Therefore, based on the position of the neutral axis (2.15), the value of the dimensionless coefficient is $\chi_2 = 0.46774$. The results of the calculations are specified in Table 2.

Table 2. The results of the analytical calculations for the exemplary beam B-2.

λ	10.0	12.5	15.0
k_s	0.4813	0.4877	0.4923
C_{se}	0.06438	0.04133	0.02876
$\widetilde{v}_{\max}$	317.53	606.75	1035.81
$\widetilde{\tau}_{\max}$	0.6123	0.6133	0.6139

- Beam B-3.

Young's modulus of the upper part of the beam is variable according to the function (2.2) – Fig. 4 ($E_1 = E_f = 70$ GPa, $\nu = 0.3$ – sandwich beam). Therefore, from the position of the neutral axis (2.15), the value of the dimensionless coefficient is $\chi_2 = 0.48530$. Thus, the neutral axis, in this case, is located at the center of the beam depth. The results of the calculations are specified in Table 3.

Table 3. The results of the analytical calculations for the exemplary beam B-3.

λ	10.0	12.5	15.0
k_s	0.1743	0.1803	0.1846
C_{se}	0.1116	0.07157	0.04976
$\widetilde{v}_{\max}$	1254.44	2361.79	3998.11
$\widetilde{\tau}_{\max}$	0.5442	0.5453	0.5462

4. Numerical FEM calculations – validation of the analytical model

FEM analyses were conducted using the ABAQUS 6.12 software for the identical set of three beams investigated analytically. Considering the beams' symmetry and applied loads, calculations were performed for halves of the structures. Boundary conditions and loads were consistent with the analytical three-point bending model, with respect to the neutral surfaces of the beams. Analytically determined dimensionless coefficients χ_1 and χ_2 were employed to establish the positions of the neutral surfaces. To account for the variability of Young's modulus, according to expression (2.2), the numerical model was divided into layers, each characterized as isotropic and linearly elastic relative to its mid-plane. A quadratic brick element C3D20R was employed for discretizing the beam model. In regions with significant variations in Young's modulus, the number of elements along the beam depth was increased. Determination of the appropriate number and thickness of layers considered solution convergence and problem

size during preliminary simulations. The numerical models, represented by FEM meshes and corresponding boundary conditions for the three beams under consideration, are depicted in Fig. 5. A comparative analysis of results obtained from the analytical and numerical calculations is presented in Tables 4–6 and Fig. 6.

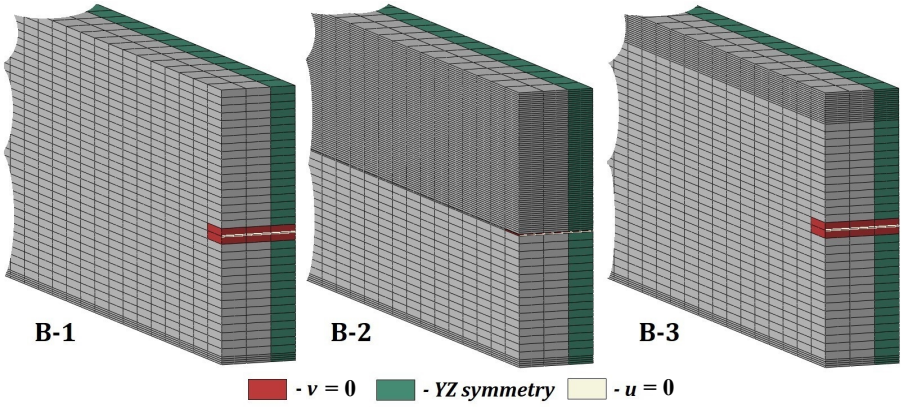

FIG. 5. The FEM meshes and boundary conditions of the beams' ends with fixed translations along the x axis.

Table 4. The comparison of analytical and FEM results for exemplary beam B-1.

λ		10.0	12.5	15.0
$\widetilde{v}_{\max}$	Analytical	200.00	385.57	661.49
	FEM	199.59	384.73	660.25
	Δ [%]	0.21	0.22	0.19
$\widetilde{\tau}_{\max}$	Analytical	0.6859	0.6877	0.6889
	FEM	0.6951	0.6951	0.6952
	Δ [%]	1.34	1.07	0.91

Table 5. The comparison of analytical and FEM results for exemplary beam B-2.

λ		10.0	12.5	15.0
$\widetilde{v}_{\max}$	Analytical	317.53	606.75	1035.81
	FEM	313.60	601.73	1029.72
	Δ [%]	1.24	0.83	0.59
$\widetilde{\tau}_{\max}$	Analytical	0.6123	0.6133	0.6139
	FEM	0.6159	0.6168	0.6168
	Δ [%]	0.60	0.57	0.47

Table 6. The comparison of analytical and FEM results for exemplary beam B-3.

λ		10.0	12.5	15.0
$\widetilde{v}_{\max}$	Analytical	1254.44	2361.79	3998.11
	FEM	1232.04	2332.57	3962.32
	Δ [%]	1.79	1.24	0.90
$\widetilde{\tau}_{\max}$	Analytical	0.5442	0.5453	0.5462
	FEM	0.5568	0.5580	0.5580
	Δ [%]	2.32	2.32	2.16

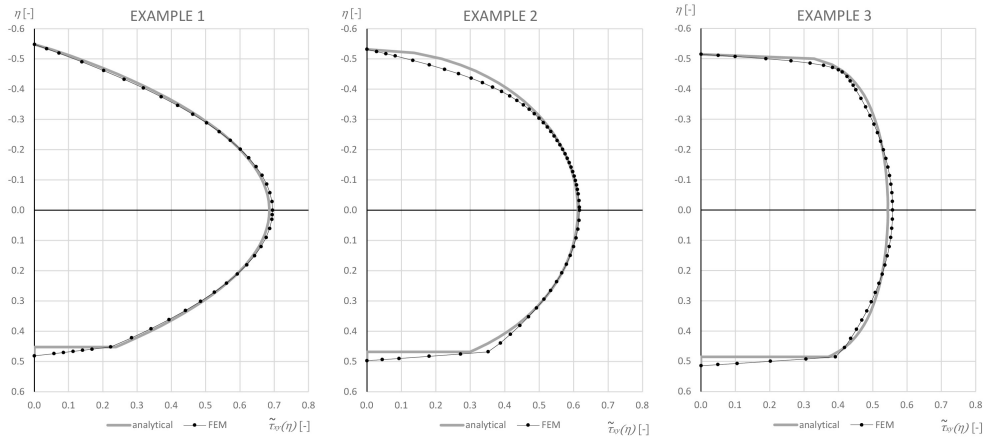

FIG. 6. The distribution of the maximal shear stresses in the depth direction of the considered beams for $\xi = 1/4$.

The above dimensionless maximum deflection and dimensionless maximum shear stress values were compared to those obtained analytically and specified in Tables 1–3, demonstrating good convergence between both sets of results. The differences between the deflection values were found to be less than 1.24%, whereas the differences between the shear stress values did not exceed 2.32%.

5. Conclusions

The following conclusions can be formulated based on the presented analytical and numerical studies of three-point bending of the beam with a non-homogeneous structure in its depth direction:

- The assumed function of Young's modulus variability along the depth of the beam (2.2) was used as a material generalization for non-symmetric beams, ranging from homogeneous to approaching sandwich structures.

- Comparisons between the analytical and numerical results of dimensionless maximum deflections and shear stresses showed good compliance, with noticeable decrease in relative differences as the relative length of the beam increased.
- The obtained distributions of shear stresses, resulting directly from the nonlinear hypothesis of deformation of the planar cross-section (2.4), were consistent with the numerical results. This confirms the accuracy of the model and allows for the consideration of shear effects, which are neglected in classical beam theory.

References

1. Manjunatha B.S., Kant T., New theories for symmetric/unsymmetric composite and sandwich beams with C^0 finite elements, *Composite Structures*, **23**(1): 61–73, 1993, doi: 10.1016/0263-8223(93)90075-2.
2. Reddy J.N., Analysis of functionally graded plates, *International Journal of Numerical Methods in Engineering*, **47**(1–3): 663–684, 2000, doi: 10.1002/(SICI)1097-0207(20000110/30)47:1/3<663::AID-NME787>3.0.CO;2-8.
3. Reddy J.N., *Mechanics of Laminated Composite Plates and Shells: Theory and Analysis*, 2nd ed., CRC Press, Boca Raton, London, New York, Washington, 2004.
4. Zenkour A.M., Generalized shear deformation theory for bending analysis of functionally graded plates, *Applied Mathematical Modelling*, **30**(1): 67–84, 2006, doi: 10.1016/j.apm.2005.03.009.
5. Altenbach H., Eremeyev V.A., Direct approach-based analysis of plates composed of functionally graded materials, *Archive of Applied Mechanics*, **78**(10): 775–794, 2008, doi: 10.1007/s00419-007-0192-3.
6. Shen H.S., *Functionally Graded Materials: Nonlinear Analysis of Plates and Shells*, CRC Press, Boca Raton, 2009.
7. Carrera E., Brischetto S., A survey with numerical assessment of classical and refined theories for the analysis of sandwich plates, *Applied Mechanics Reviews*, **62**(1): 010803, 2009, doi: 10.1115/1.3013824.
8. Carrera E., Giunta G., Petrolo M., *Beam Structures. Classical and Advanced Theories*, John Wiley & Sons, Ltd., 2011.
9. Lezgy-Nazargah M., Shariyat M., Beheshti-Aval S.B., A refined high-order global-local theory for finite element bending and vibration analyses of laminated composite beams, *Acta Mechanica*, **217**(3): 219–242, 2011, doi: 10.1007/s0070701003919.
10. Weps M., Naumenko K., Altenbach H., Unsymmetric three-layer laminate with soft core for photovoltaic modules, *Composite Structures*, **105**: 332–339, 2013, doi: 10.1016/j.compstruct.2013.05.029.
11. Zenkour A.M., A simple four-unknown refined theory for bending analysis of functionally graded plates, *Applied Mathematical Modelling*, **37**(20–21): 9041–9051, 2013, doi: 10.1016/j.apm.2013.04.022.

12. Magnucki K., Smyczyński M., Jasion P., Deflection and strength of a sandwich beam with thin binding layers between faces and a core, *Archives of Mechanics*, **65**(4): 301–311, 2013.

13. Chen D., Yang J., Kitipornchai S., Elastic buckling and static bending of shear deformable functionally graded porous beam, *Composite Structures*, **133**: 54–61, 2015, doi: 10.1016/j.compstruct.2015.07.052.

14. Sayyad A.S., Ghugal Y.M., Bending, buckling and free vibration of laminated composite and sandwich beams: a critical review of literature, *Composite Structures*, **171**: 486–504, 2017, doi: 10.1016/j.compstruct.2017.03.053.

15. Vo T.P., Thai H.-T., Nguyen T.-K., Lanc D., Karamanli A., Flexural analysis of laminated composite and sandwich beams using a four-unknown shear and normal deformation theory, *Composite Structures*, **176**: 388–397, 2017, doi: 10.1016/j.compstruct.2017.05.041.

16. Abrate S., Di Sciuva M., Equivalent single layer theories for composite and sandwich structures: a review, *Composite Structures*, **179**: 482–494, 2017, doi: 10.1016/j.compstruct.2017.07.090.

17. Magnucka-Blandzi E., Kędzia P., Smyczyński M., Unsymmetrical sandwich beams under three-point bending – Analytical studies, *Composite Structures*, **202**: 539–544, 2018, doi: 10.1016/j.compstruct.2018.02.086.

18. Magnucki K., Lewiński J., Magnucka-Blandzi E., Kędzia P., Bending, buckling and free vibration of a beam with unsymmetrically varying mechanical properties, *Journal of Theoretical and Applied Mechanics*, **56**(4): 1163–1178, 2018, doi: 10.15632/jtam-pl.56.4.1163.

19. Magnucki K., Witkowski D., Magnucka-Blandzi E., Buckling and free vibrations of rectangular plates with symmetrically varying mechanical properties – Analytical and FEM studies, *Composite Structures*, **220**: 355–361, 2019, doi: 10.1016/j.compstruct.2019.03.082.

20. Sayyad A.S., Ghugal Y.M., Modeling and analysis of functionally graded sandwich beams: A review, *Mechanics of Advanced Materials and Structures*, **26**(21): 1776–1795, 2019, doi: 10.1080/15376494.2018.1447178.

21. Meksi R., Benyoucef S., Mahmoudi A., Tounsi A., Bedia E.A.A., Mahmoud S.R., An analytical solution for bending, buckling and vibration responses of FGM sandwich plates, *Journal of Sandwich Structures and Materials*, **21**(2): 727–757, 2019, doi: 10.1177/1099636217698443.

22. Magnucki K., Magnucka-Blandzi E., Lewiński J., Milecki S., Analytical and numerical studies of an unsymmetrical sandwich beam – bending, buckling and free vibration, *Engineering Transactions*, **67**(4): 491–512, 2019, doi: 10.24423/EngTrans.1015.20190725.

23. Genovese D., Elishakoff I., Shear deformable rod theories and fundamental principles of mechanics, *Archive of Applied Mechanics*, **89**(10): 1995–2003, 2019, doi: 10.1007/s00419-019-01556-7.

24. Magnucki K., Lewinski J., Magnucka-Blandzi E., Bending of two-layer beams under uniformly distributed load – Analytical and numerical FEM studies, *Composite Structures*, **235**: 111777, 2020, doi: 10.1016/j.compstruct.2019.111777.

25. Magnucki K., Lewinski J., Magnucka-Blandzi E., An improved shear deformation theory for bending beams with symmetrically varying mechanical properties in the depth direction, *Acta Mechanica*, **231**(10): 4381–4395, 2020, doi: 10.1007/s00707-020-02763-y.

26. Malikan M., Eremeyev V.A., A new hyperbolic-polynomial higher-order elasticity theory for mechanics of thick FGM beams with imperfection in the material composition, *Composite Structures*, **249**: 112486, 2020, doi: 10.1016/j.compstruct.2020.112486.

27. Malikan M., Eremeyev V.A., The effect of shear deformations' rotary inertia on the vibrating response of multi-physics composite beam-like actuators, *Composite Structures*, **297**: 115951, 2020, doi: 10.1016/j.compstruct.2020.115951.

28. Sedighi H.M., Malikan M., Valipour A., Żur K.K., Nonlocal vibration of carbon/boron-nitride nano-hetero-structure in thermal and magnetic fields by means of nonlinear finite element method, *Journal of Computational Design and Engineering*, **7**(5): 591–602, 2020, doi: 10.1093/jcde/qwaa041.

29. Masjedi P.K., Weaver P.M., Variable stiffness composite beams subject to non-uniformly distributed loads: An analytical solution, *Composite Structures*, **256**: 112975, 2021, doi: 10.1016/j.compstruct.2020.112975.

30. Garg A., Belarbi M.-O., Chalak H.D., Chakrabarti A., A review of the analysis of sandwich FGM structures, *Composite Structures*, **258**: 113427, 2021, doi: 10.1016/j.compstruct.2020.113427.

31. Magnucki K., Magnucka-Blandzi E., Wittenbeck L., Three models of a sandwich beam: bending, buckling and free vibrations, *Engineering Transactions*, **70**(2): 97–122, 2022, doi: 10.24423/EngTrans.1416.20220331.

Received January 17, 2023; accepted version October 5, 2023.